SCIPP 93/44
November 1993

Fermilab Library
0 1160 0026710 8
SCIPP-93-44

Review of Charm Physics*

PATRICIA R. BURCHAT
Santa Cruz Institute for Particle Physics
University of California, Santa Cruz, CA 95064

Abstract

Experimental studies of charm decays are reviewed with particular emphasis on recent measurements of absolute branching fractions, purely leptonic decay rates, semileptonic decay rates and form factors, the D_s lifetime, $D^0\bar{D}^0$ mixing and doubly-Cabibbo-suppressed decays.

Invited talk at the
5th International Symposium on Heavy Flavor Physics
Montreal, Canada, July 6–10, 1993

* Work supported in part by the U.S. Department of Energy and the National Science Foundation.

1 Introduction

Studies of decays of the charm quark have played a unique role in particle physics because the charm quark is the lightest of the "heavy" quarks and is more easily accessible to experimenters. Measurements of particular aspects of heavy quark decays are usually made first for the charm quark and later for the bottom quark. Because many more hadrons have been produced containing the charm quark than the bottom quark, the measurements are usually more precise in the charm sector.

The precision of charm quark studies continues to increase as larger samples of charmed particles become available, the largest of which are summarized in Tables 1 and 2 for e^+e^- colliding-beam and fixed-target experiments, respectively. The Mark III experiment was designed specifically to study charm quark decays at the SPEAR e^+e^- storage ring. Now each experiment at LEP has recorded almost an order of magnitude more charm decays while CLEO II has recorded about two orders of magnitude more.

Table 1 Summary of charm samples produced in e^+e^- colliding beam experiments

Experiment	$\sqrt{S}$	$\int \mathcal{L}dt$	Produced Charm
Mark III	3.77 GeV	9 pb^{-1}	28,000 $D^0\bar{D}^0$ 20,000 D^+D^-
	4.14 GeV	6 pb^{-1}	3,000 $D_s\bar{D}_s$
BES	4.03 GeV	9 pb^{-1}	6,000 $D_s\bar{D}_s$
CLEO II	$\sim$ 10 GeV	1.8 fb^{-1} analysed	2×10^6 $D\bar{D}$
LEP	$\sim$ 90 GeV	10^6 Z's per experiment	200,000 $c\bar{c}$ per experiment
SLC	$\sim$ 90 GeV	50×10^3 Z's	10,000 $c\bar{c}$

The photoproduction experiment E691 at Fermilab was the first experiment to conduct precise charm studies in the fixed-target environment. E691 and Mark III had comparable numbers of fully reconstructed charm decays. However, E691 had the advantage of measuring the decay time of each charm decay with an uncertainty considerably less than the mean lifetime due to the large boost the charmed hadrons receive in a fixed target experiment. This allowed E691 to discriminate the charm decays from the significant light-quark background and to make precise charmed lifetime measurements. More recently, the photoproduction experiment E687 and

Table 2 Summary of charm samples fully reconstructed in fixed target-experiments.

Experiment	Date of Completion	# of Events Recorded	# of Fully Reconstructed Charm Decays
photoproduction			
E691	Aug., 1985	100×10^6	10,000
E687	Jan., 1992	500×10^6	80,000
hadroproduction			
WA75		2×10^6	350
NA32	Aug., 1986	17×10^6	1,300
(ACCMOR)			
WA82	Sept., 1989	10×10^6	3,000
E653	Feb., 1988	10×10^6	1,000
E769	Feb., 1988	500×10^6	4,000
E791	Jan., 1992	$20,000 \times 10^6$	200,000

the hadroproduction experiment E791 (both at Fermilab) have accumulated large samples of charm decays and have demonstrated charm signals corresponding to about 8 and 20 times the E691 sample, respectively, with comparable signal-to-background ratios.

Also listed in Table 2 are several fixed target experiments in which significantly fewer events were recorded compared to E691, E687 or E791, but in which a specialized trigger and/or detector allowed the experiment to make significant contributions for particular decay modes. For example, the WA75 experiment at CERN and E653 at Fermilab both had emulsion targets and muon triggers. Both experiments have recently shown evidence for the purely leptonic decay $D_s \to \mu\nu$ as discussed later in this review.

This review includes significant results that have been published in the past year, and new results submitted to this and recent conferences. The emphasis is on studies of charmed meson decays including absolute branching fractions, purely leptonic decays, semileptonic decays, D_s lifetime, $D^0\bar{D}^0$ mixing and doubly-Cabibbo-suppressed decays. Although progress has been made in the areas of charmed meson and baryon spectroscopy, hadronic decays, rare decays and baryon lifetimes, these topics are not covered in this review. For a recent review which includes some of these topics, see reference 1.

2 D^* Branching Fractions and Isospin Mass Splitting

In 1992, CLEO II published measurements of $D^*(2010)$ branching fractions to $D\gamma$ and $D\pi$, and $D^* - D$ mass differences. These studies demonstrate how the excellent photon reconstruction capabilities afforded by the CLEO II CsI(Tl) crystal calorimeter enable measurements to be made in the charm sector that were previously unattainable. In addition, these measurements are relevant in some of the more recent analyses.

The CLEO II results [2] and the 1992 Particle Data Group world averages [3] for the D^* branching ratios are shown in Table 3. In the CLEO II measurement, the branching fractions of each D^* state are constrained to add up to 1 and isospin conservation is used to relate $B(D^{*+} \to D^+\pi^0)$ to $B(D^{*+} \to D^0\pi^+)$. Therefore, only the relative rates for modes containing a D and a π^0 or γ have to be measured, reducing systematic uncertainties on the results. This measurement depends on CLEO II's ability to reconstruct the low-energy photons and π^0's from D^* decays. The most significant difference in results compared to previous measurements is in the branching fraction for $D^{*+} \to D^+\gamma$. The new result is in much better agreement with theoretical expectations [4] than the old result which was dominated by a Mark III measurement. [5]

Table 3 $D^*(2010)$ branching fractions measured by CLEO II compared to the 1992 Particle Data Group (PDG) world averages

	Branching Fraction (%)	
Decay mode	CLEO II [2]	1992 PDG [3]
$D^{*+} \to D^+\gamma$	$1.1 \pm 1.4 \pm 1.6$	18 ± 4
$D^{*+} \to D^+\pi^0$	$30.8 \pm 0.4 \pm 0.8$	27.2 ± 2.5
$D^{*+} \to D^0\pi^+$	$68.1 \pm 1.0 \pm 1.3$	55 ± 4
$D^{*0} \to D^0\gamma$	$36.4 \pm 2.3 \pm 3.3$	45 ± 6
$D^{*0} \to D^0\pi^0$	$63.6 \pm 2.3 \pm 3.3$	55 ± 6

The excellent photon identification capabilities were also used to measure the mass splitting for $D^{*+} - D^+$ and for $D^{*0} - D^0$. [6] These results are shown in Table 4 along with the world average value for the $D^{*+} - D^0$ mass splitting which is dominated by an ACCMOR measurement. From these three numbers, the $D^{*+} - D^{*0}$ and the $D^+ - D^0$ mass splittings are determined and are also shown in the Table. Finally, the difference in D^* and D mass splittings is determined: $(M_{D^+} - M_{D^0}) - (M_{D^{*+}} - M_{D^{*0}}) = (1.48 \pm 0.09 \pm 0.05)$ MeV. This mass splitting depends on the wave function overlap at the origin $|\psi(0)|^2$. Since the D decay constant f_D (see

Sec. 4) also depends on $|\psi(0)|^2$, measurements of the mass splitting and the decay constant in the charm sector can be used to improve theoretical models. These models could then be used to derive a value for f_B from isospin mass difference measurements in the B system.

Table 4 Measurements of $D^* - D$ mass splittings and other derived splittings

	Mass Difference (MeV)	Source
$D^{*+} - D^+$	$140.64 \pm 0.08 \pm 0.06$	CLEO II [6]
$D^{*0} - D^0$	$142.12 \pm 0.05 \pm 0.05$	CLEO II [6]
$D^{*+} - D^0$	145.44 ± 0.06	PDG [3]
$D^{*+} - D^{*0}$	$3.32 \pm 0.08 \pm 0.05$	derived
$D^+ - D^0$	$4.80 \pm 0.10 \pm 0.06$	derived

3 Absolute Branching Fractions of D^+ and D^0

ALEPH and CLEO II both report new measurements of absolute branching fractions for D decays. Historically, three methods have been used to measure the D absolute branching fractions.

1. The Mark III collaboration [7] used the relative number of events with two fully reconstructed and one fully reconstructed charm decay(s) to extract the absolute branching fractions.
2. The ACCMOR collaboration [8] used a unitarity constraint to extract the absolute branching fractions. That is, they required the sum of the branching fractions for the observed modes to sum to $1 - f$ where f is the branching fraction to modes *not* observed. This method relies on estimating f for both D^0 and D^+ decays.
3. The HRS collaboration [9] pioneered a method that uses the low-momentum charged pions from $D^{*+} \to D^0\pi^+$ for normalization. They searched for fully reconstructed D^0 decay candidates associated with a slow charged pion and used the total number of slow pions as a measure of the total number of produced D^0's from D^{*+} decays. The correlation between the direction of the slow pion and the direction of the D^{*+} (estimated by the jet axis) was used as a discriminator between slow pions from D^* decay and other pions produced in the event.

The ALEPH [10] experiment used the third method to measure the absolute branching fraction for $D^0 \to K^-\pi^+$. ALEPH now has a new measurement [11] with a comparable statistical error but a smaller systematic error. The distribution of the pion momentum transverse to the jet axis, p_t, was studied for six laboratory momentum ranges between 1.5 and 4 GeV/c. An excess near $p_t = 0$ is ascribed to pions from D^{*+} decays and is used to provide the normalization for the absolute branching fraction of $D^0 \to K^-\pi^+$. The old ALEPH measurement was $(3.62 \pm 0.34 \pm 0.44)\%$; the new measurement is $(3.89 \pm 0.29 \pm 0.16)\%$.

CLEO II [12] has extended the third method to measure the absolute branching fraction for both $D^0 \to K^-\pi^+$ and $D^+ \to K^-\pi^+\pi^+$ using slow π^+'s *and* low energy π^0's to tag D^* decays. For the measurement of $B(D^0 \to K^-\pi^+)$, charged pions with laboratory momentum between 225 and 425 MeV/c are used. CLEO II uses the distribution of $\sin^2\theta$ where θ is the angle between the jet thrust axis and the slow pion, rather than p_t, to discriminate slow pions from D^{*+} decay and slow pions from other processes. The distribution of $\sin^2\theta$ for the background is determined using pions in the *opposite* jet with the *same* charge as the tagged pion in the D^* decay. The distribution of $\sin^2\theta$ for the slow pions and the contribution from background are shown in Figure 1. The branching fraction, extracted by comparing the number of reconstructed $D^0 \to K^-\pi^+$ decays with a slow pion to the total number of slow pions from $D^{*+} \to D^0\pi^+$ decay, is $(3.91 \pm 0.08 \pm 0.17)\%$.

The measurement of the absolute branching fraction for a D^+ decay is more complicated since there are two sources of slow π^0's: the decay $D^{*+} \to D^+\pi^0$ which provides the normalization for D^+ absolute branching fractions, and $D^{*0} \to D^0\pi^0$. The extraction of $B(D^+ \to K^-\pi^+\pi^+)$ involves using all of the following:

1. a measurement of *both* the slow π^+ rate from $D^{*+} \to D^0\pi^+$ and the low energy π^0 rate from $D^{*0} \to D^0\pi^0$ with $D^0 \to K^-\pi^+$;
2. the measurement of $B(D^0 \to K^-\pi^+)$ described above;
3. the ratio $B(D^{*+} \to D^0\pi^+)/B(D^{*+} \to D^+\pi^0)$ from isospin conservation;
4. the ratio of efficiencies for reconstructing the slow π^0 and the slow π^+, *extracted from the data itself.* Both the statistical and systematic uncertainties on $B(D^+ \to K^-\pi^+\pi^+)$ are dominated by the uncertainty on this ratio of efficiencies.

Both old and new measurements of $B(D^0 \to K^-\pi^+)$ and $B(D^+ \to K^-\pi^+\pi^+)$ are summarized in Table 5. From these measurements, the average branching fractions are $B(D^0 \to K^-\pi^+) = (3.96 \pm 0.14)\%$ and $B(D^+ \to K^-\pi^+\pi^+) = (8.98 \pm 0.83)\%$. The fractional error for the D^0 decay mode is now less than 5% while the fractional error for the D^+ mode is about 10%.

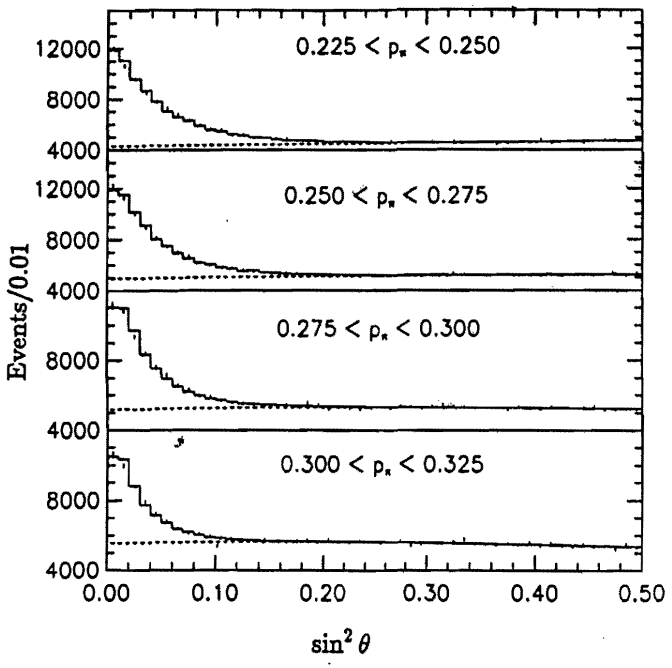

Figure 1 Distribution of the angle θ between the slow pion and the jet axis for four equal intervals of pion momentum between 225 and 325 MeV/c. Eight intervals between 225 and 425 MeV/c were used in the analysis. The points correspond to the data. The solid histogram represents a fit that includes signal and background contributions. The dashed curve represents the contribution from background alone. Note the suppressed zero on the vertical scale.

Table 5 Measurements of the absolute branching fractions for $D^0 \to K^-\pi^+$ and $D^+ \to K^-\pi^+\pi^+$

Experiment	$B(D^0 \to K^-\pi^+)$ (%)	$B(D^+ \to K^-\pi^+\pi^+)$ (%)
Mark III [7]	$4.2 \pm 0.4 \pm 0.4$	$9.1 \pm 1.3 \pm 0.4$
ACCMOR [8]	$3.75^{+0.44}_{-0.41}$	8.0 ± 1.4
HRS [9]	$4.5 \pm 0.8 \pm 0.5$	
ARGUS [13]	$4.33 \pm 0.15 \pm 0.40$	
ALEPH (1993) [11]	$3.89 \pm 0.29 \pm 0.16$	
CLEO II (1993) [12]	$3.91 \pm 0.08 \pm 0.17$	$10.0 \pm 1.0 \pm 1.2$
Average	3.96 ± 0.14	8.98 ± 0.83

4 Purely Leptonic Decays

The simplest decays of charmed mesons to interpret theoretically are the purely leptonic decays. This year, positive evidence for the decay $D_s \to \mu\nu$ has been reported by several experiments. The decay rate for a charged D meson to decay leptonically is given by

$$\Gamma(D \to l^+\nu_l) = \frac{G_F^2 f_D^2}{8\pi}|V_{cq}|^2 m_l^2 m_D (1 - \frac{m_l^2}{m_D^2})^2$$

where f_D is the *decay constant* which contains the effects of the strong interaction (in the binding of the quarks in the D meson), V_{cq} is the Kobayashi-Maskawa matrix element, and m_l and m_D are the masses of the lepton and D meson, respectively. The factor of m_l^2 in the decay rate is the helicity suppression factor that strongly suppresses the decay $D \to e\nu_e$. If we know V_{cq}, a measurement of the decay rate for a purely leptonic mode allows us to determine f_D which is important for the following reasons.

1. It measures the $c\bar{q}$ wavefunction overlap in the D meson.
2. It appears in numerous heavy-flavor transitions such as those in mixing and CP violation.
3. It provides an important test of non-perturbative QCD calculations (QCD-inspired potential models, QCD sum rules, lattice calculations, *etc.*).

The calculated values for f_D and f_{D_s} are approximately 200 MeV and 230 MeV, respectively. Using these values for the decay constants, the values of the CKM matrix elements from the Particle Data Group [3] ($|V_{cd}| = 0.22$ and $|V_{cs}| = 0.97$), and the measured D^+ and D_s lifetimes, we obtain the approximate branching fraction expectations shown in Table 6. The purely leptonic decay rates for D_s are expected to be larger than those for D^+ because $|V_{cs}|^2$ is much larger than $|V_{cd}|^2$. In addition, the decay $D_s \to \tau\nu_\tau$ has less phase-space suppression than $D^+ \to \tau\nu_\tau$. Therefore, the decay modes that are most likely to be detected experimentally are $D_s \to \mu\nu_\mu$ and $D_s \to \tau\nu_\tau$.

The Mark III collaboration [14] set an upper limit of 7.2×10^{-4} on $B(D^+ \to \mu^+\nu_\mu)$, corresponding to an upper limit of 290 MeV on f_D. The EMC collaboration [15] set an upper limit of 3% on $B(D_s \to \mu^+\nu_\mu)$. This result depends on the assumption that the D_s production rate is 20% of the total charm production rate.

In 1992, the CERN WA75 collaboration [16] presented the first observation of the muonic decay $D_s \to \mu^+\nu_\mu$. In this fixed-target experiment, a π^- beam was incident on an emulsion target. A muon with significant momentum transverse to the beamline was required in both the online trigger and in the offline analysis.

Table 6 Calculated purely-leptonic branching fractions under the following assumptions: $f_D = 200$ MeV, $f_{D_s} = 230$ MeV, $|V_{cd}| = 0.22$ and $|V_{cs}| = 0.97$

Decay Mode	Rate (s^{-1})	Branching Fraction
$D^+ \to e^+\nu_e$	8×10^3	8×10^{-9}
$D^+ \to \mu^+\nu_\mu$	3×10^8	3×10^{-4}
$D^+ \to \tau^+\nu_\tau$	9×10^8	9×10^{-4}
$D_s \to e^+\nu_e$	2×10^5	9×10^{-8}
$D_s \to \mu^+\nu_\mu$	9×10^9	4×10^{-3}
$D_s \to \tau^+\nu_\tau$	9×10^{10}	4×10^{-2}

The line of flight of the decaying charmed hadron was determined in emulsion through scanning. The momentum of the muon transverse to this direction p_t^μ was then determined. The kinematic upper limit for p_t^μ is 0.98 GeV/c for $D_s \to \mu\nu_\mu$ and 0.93 GeV/c for $D^+ \to \mu\nu_\mu$, while the upper limit for semileptonic decays is about 0.88 GeV/c. Six events were observed with $p_t^\mu > 0.9$ GeV/c. Using the signal for $D^0 \to \mu\nu_\mu X$ for normalization, the WA75 collaboration determines a branching fraction for $D_s \to \mu\nu_\mu$ of $(4.0^{+1.8+0.8}_{-1.4-0.6} \pm 1.7) \times 10^{-3}$ and a D_s decay constant of $f_{D_s} = (232 \pm 45 \pm 20 \pm 48)$ MeV where in both results the third error is the systematic error on the normalization which depends on measurements of the D_0 and D_s cross-sections from NA32 and the inclusive semileptonic branching fractions from Mark III. The E653, CLEO II and BES collaborations all have new or preliminary evidence for purely leptonic D_s decays. Like WA75, E653 [17] is a fixed target experiment with an emulsion target and muon trigger. The spectrum of the muon momentum with respect to the direction of the D_s, p_t^μ, is shown in Figure 2. In a partial data sample, 23 events are observed with high p_t^μ. Approximately three times as many events are expected from a scan of the full data sample. The collaboration will normalize to the $D_s \to \phi\mu\nu_\mu$ signal in the same data sample to extract a branching ratio. The E653 collaboration also observes three candidates (in a partial data set) for $D_s \to \tau\nu_\tau$ decay in which $\tau \to \mu\nu_\mu\bar{\nu}_\tau$. In these events, both the decay of the D_s and the decay of the τ occur in the emulsion.

The CLEO II collaboration [18] searches for $\mu\gamma$ combinations from the decay chain $D_s^* \to D_s\gamma$, $D_s \to \mu\nu_\mu$. The neutrino momentum is estimated from the missing energy and momentum in the hemisphere of the muon and is used, along with the measured μ and γ momentum, to determine the candidate D_s and D_s^* mass. The distribution for the mass difference $m(\mu\nu_\mu\gamma) - m(\mu\nu_\mu)$ is shown in Figure 3. The signal should peak at $m(D_s^*) - m(D_s) \approx 141$ MeV. Most of the

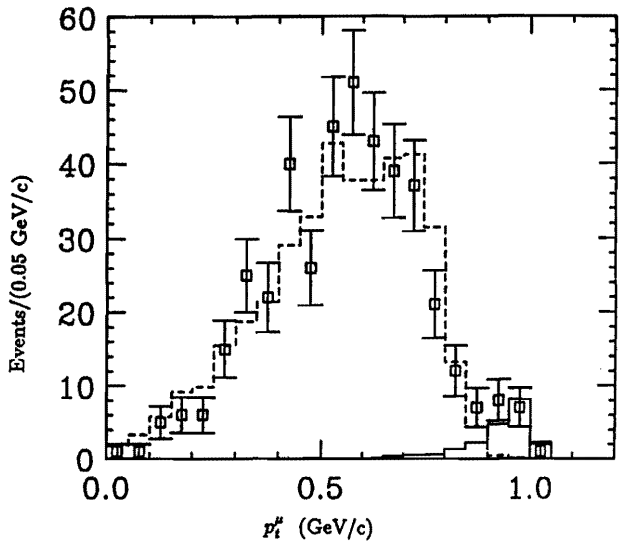

Figure 2 Distribution of the muon momentum with respect to the D direction as measured in the emulsion in experiment E653. The points correspond to the data. The dashed and solid histograms represent a Monte Carlo simulation of the expected signal shapes for $D^+ \to \bar{K}^0\mu^+\nu_\mu$ and $D_s \to \mu^+\nu_\mu$, respectively.

entries in Figure 3 are due to other sources of muons and γ's. To account for these sources, the same analysis is done with electrons instead of muons. The electron data is represented by the dashed histogram in Figure 3. The difference between the mass-difference distribution for muons and electrons is shown in Figure 4 and is attributed to the decay $D_s \to \mu\nu_\mu$. The distribution is fit to a combination of a Gaussian peak at 141 MeV and a background due to $D_s \to \mu\nu_\mu$ decays combined with random γ's. The result of the fit is 38 events from the first source and 52 events from the second. The branching fraction is measured relative to the $\phi\pi^+$ decay mode: $B(D_s \to \mu\nu_\mu)/B(D_s \to \phi\pi^+) = 0.245 \pm 0.052 \pm 0.074$. Using the value $B(D_s \to \phi\pi^+) = (3.7 \pm 0.9)\%$ (see next section), they extract a decay constant of $f_{D_s} = 344 \pm 37 \pm 52 \pm 42$ MeV where the last error is due to the uncertainty in the branching fraction $B(D_s \to \phi\pi^+)$.

Finally, among approximately 3500 produced $e^+e^- \to D_s^+D_s^-$ events, the BES collaboration has fully reconstructed one candidate event with $D_s^+ \to K^{*0}K^+$ and $D_s^- \to \mu^-\nu_\mu$. The missing mass in the event is consistent with zero.

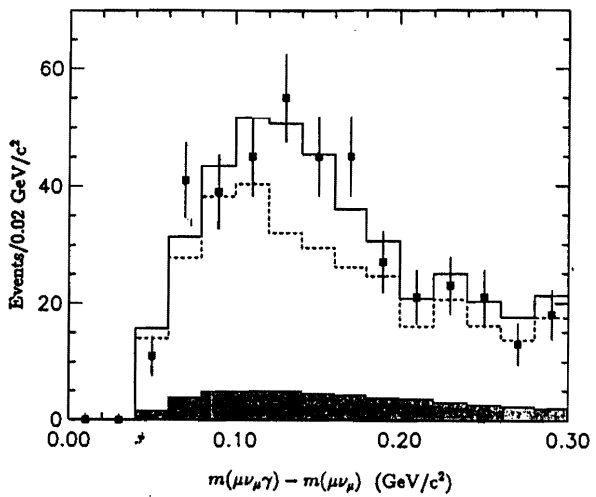

Figure 3 Distribution of the mass difference $m(\mu\nu\gamma) - m(\mu\nu)$ for candidates for the decay sequence $D_s^* \to D_s\gamma$, $D_s \to \mu\nu_\mu$ in the CLEO II data. The points represent muon data. The dashed histogram represents backgrounds estimated with electrons plus a small component represented by the shaded histogram due to differences in the electron and muon misidentification rate.

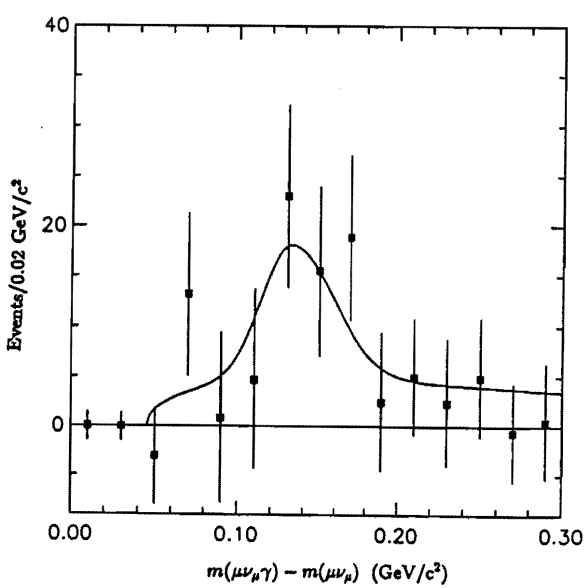

Figure 4 The difference between the points and the dashed histogram in the previous figure are ascribed to $D_s \to \mu\nu$ candidates and are represented by the points in this figure. The solid line corresponds to a fit to an asymmetric Gaussian from real $D_s^* \to D_s\gamma$, $D_s \to \mu\nu$ decays, plus a contribution from $D_s \to \mu\nu$ decays combined with a random photon.

5 Semileptonic Decays

Semileptonic decays are the next simplest of charm decays to interpret. The parts of the matrix element describing the leptonic and hadronic vertices factorize. The leptonic current can be calculated exactly and the hadronic current can be written in terms of form factors that contain the effects of the strong interaction. Studies of semileptonic decays can be used to extract the form factors or the CKM matrix elements describing the quark couplings to the W. Measurements of the form factors can be used to test predictions of quark model calculations, lattice gauge calculations, QCD sum rules or the heavy quark effective theory.

In this section, I first discuss semileptonic D decays with a pseudoscalar meson in the final state. I then turn to the more complicated case of semileptonic decays with a vector meson in the final state.

5.1 $D^0 \to K^- l^+ \nu_l$

The differential decay rate for $D^0 \to K^- l^+ \nu_l$ can be written in terms of one form factor $f_+(q^2)$*

$$\frac{d\Gamma}{dq^2} = \frac{G_F^2 |V_{cs}|^2 p_K^3 M_D^2}{24\pi^3} |f_+(q^2)|^2,$$

where q^2 is the invariant mass of the virtual W ($q^2 = M_{l\nu}^2$). The studies of this decay have focussed on determining the q^2 dependence of the form factor and on measuring the total rate which leads to a determination of the form factor f_+ at a particular q^2 assuming the q^2 dependence is known.

Measurements of the relative D^0 branching fractions to the semileptonic mode $K^- l^+ \nu_l$ and to the hadronic mode $K^-\pi^+$ are shown in Table 7. The E687 result is preliminary, based on 30% of their data sample. The new CLEO II result [19] is based on 2700 candidates for $D^0 \to K^- l \nu_l$ with $l = e$ or μ.

Since the sample of $D^0 \to K^- l^+ \nu_l$ decay candidates from CLEO II is significantly larger than any previous sample, the analysis will be described in more detail here. Leptons are identified and accepted if the momentum in the laboratory frame is greater than 0.7 GeV for electrons, and above 1.4 GeV for muons. The decay $D^{*+} \to D^0\pi^+$ is used to obtain a clean sample of $K^- l \nu_l$ decays just as it is often used to obtain a clean sample of $K^-\pi^+$ decays. The only difference is that the neutrino is not detected, thus broadening the peak in the distribution of mass difference $\delta m = m(Kl\pi) - m(Kl)$.

* There is an additional form factor, referred to as $f_-(q^2)$, whose contribution goes to zero as the lepton mass approaches zero.

Table 7 Experimental measurements of the branching ratio $B(D^0 \to K^- l^+ \nu_l)/B(D^0 \to K^- \pi^+)$ and of the quantity M_P (described in the text) which is used to parametrize the q^2 dependence of the form factor $f_+(q^2)$

Experiment	Lepton Type	# of Events	$\frac{B(D^0 \to K^- l^+ \nu_l)}{B(D^0 \to K^- \pi^+)}$	M_P (GeV)
E691 [21]	e	250	$0.90 \pm 0.07 \pm 0.11$	$2.1 \pm 0.3 \pm 0.2$
CLEO [22]	e	584	$0.91 \pm 0.06 \pm 0.06$	$2.1 \pm 0.3 \pm 0.2$
CLEO [22]	μ	231	$0.79 \pm 0.08 \pm 0.09$	
MARK III [20]	e	56		$1.8 \pm 0.3 \pm 0.2$
E687 [23]	μ	338	$0.82 \pm 0.13 \pm 0.13$	$2.1^{+0.7+0.7}_{-0.3-0.3}$
CLEO II [19]	e, μ	2700	$0.978 \pm 0.027 \pm 0.044$	$2.00 \pm 0.12 \pm 0.18$
Average			0.931 ± 0.038	

CLEO II uses their measured value of the absolute branching fraction for $D^0 \to K^- \pi^+$ to determine $B(D^0 \to K^- l^+ \nu_l) = (3.82 \pm 0.11 \pm 0.25)\%$. The 2700 CLEO II $D^0 \to K^- l^+ \nu_l$ candidates were used to study the q^2 dependence of the form factors. There are two functional forms that are often assumed: an exponential form $f_+(q^2) = f_+(0)e^{\alpha q^2}$ and a pole form $f_+(q^2) = \frac{f_+(0)}{1-q^2/M_P^2}$. The exponential form is used, for example, in the ISGW model [24] and is predicted to be 0.21 GeV^{-2}. In the pole form, the pole mass is assumed to be the nearest $c\bar{s}$ resonance with the appropriate quantum numbers J_P. Since f_+ is a vector form factor, we expect $M_P = M_{D_s^*} = 2.1$ GeV/c^2. The two functional forms for $f_+(q^2)$ are practically indistinguishable over the accessible q^2 range.

Several experiments have attempted to measure the q^2 dependence of the form factor. The results are summarized in Table 7. All the measurements of M_P are consistent with $M_{D_s^*}$. A plot of the q^2 spectrum for the CLEO II data is shown in Figure 5. The CLEO II collaboration also fit for the parameter α. The measured value of $\alpha = (0.29 \pm 0.04 \pm 0.06)$ GeV^{-2} is about one standard deviation higher than the value used in the ISGW model. Of course, M_P and α are not independent parameters; they are related by the equation $\alpha = 1/(M_P^2 - q_{ave}^2)$ where q_{ave}^2 is the average q^2. The absolute branching fraction for $D^0 \to K^- l^+ \nu_l$ measured by CLEO II can be combined with the measured D^0 lifetime to extract a value of $f_+(0)$, assuming a form factor dependence of $f_+(q^2) = f_+(0)e^{\alpha q^2}$ and using the measured value of α. The result is $f_+(0) = 0.77 \pm 0.01 \pm 0.04$, consistent with theoretical predictions.

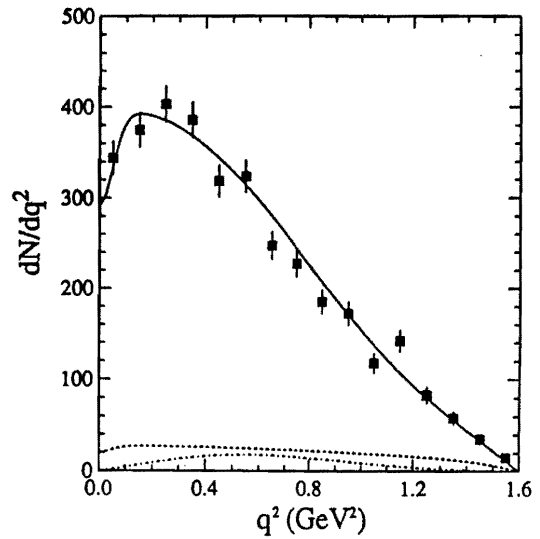

Figure 5 Distribution of q^2, the $l^+\nu_l$ invariant mass squared, for 2700 $D^0 \to K^- l^+ \nu_l$ candidates in the CLEO II data. The solid curve is the best fit. The dashed line represents the combinatorial background and the dotted line is the contribution from $K^* l\nu$ decays.

5.2 Other semileptonic decays to pseudoscalars

The CLEO II collaboration used the decay $D^{*+} \to D^+\pi^0$ to tag 160 $D^+ \to \bar{K}^0 l^+ \nu_l$ decays. The branching ratio relative to the hadronic decay $\bar{K}^0\pi^+$ was measured to be $2.60 \pm 0.35 \pm 0.26$. Assuming $\Gamma(D^0 \to K^- l^+ \nu_l) = \Gamma(D^+ \to \bar{K}^0 l^+ \nu_l)$ and using the measured D^0 and D^+ lifetimes and CLEO II's measured value of $B(D^0 \to K^- l^+ \nu_l)/B(D^0 \to K^- \pi^+)$, we can determine the ratio of hadronic branching fractions $\frac{B(D^0 \to K^- \pi^+)}{B(D^+ \to \bar{K}^0 \pi^+)} = 1.05 \pm 0.15 \pm 0.12$. This result is between one and two standard deviations lower than the Particle Data Group value [3] of 1.40 ± 0.23.

The CLEO II collaboration [25] also uses $D_s^{*+} \to D^+\pi^0$ to tag 58 Cabibbo-suppressed $D^+ \to \pi^0 l^+ \nu$ decays. The branching ratio relative to the Cabibbo-favored decay $D^+ \to \bar{K}^0 l^+ \nu_l$ was measured to be $\frac{B(D^+ \to \pi^0 l^+ \nu_l)}{B(D^+ \to \bar{K}^0 l^+ \nu_l)} = 0.085 \pm 0.027 \pm 0.014$. From this result, the following ratio of CKM matrix elements and form factors can be determined:

$$\left|\frac{V_{cd}}{V_{cs}}\right|^2 \left(\frac{f_+^\pi(0)}{f_+^K(0)}\right)^2 = 0.085 \pm 0.027 \pm 0.014.$$

This result can be compared to the Mark III measurement [26] of $0.057^{+0.038}_{-0.017} \pm 0.005$ for same quantity based on seven $D^0 \to \pi^- e^+ \nu_e$ and 56 $D^0 \to K^- e^+ \nu_e$ events. When the unitarity constraint is imposed on the CKM matrix, the ratio of CKM matrix elements is predicted to be $\left|\frac{V_{cd}}{V_{cs}}\right|^2 = 0.051 \pm 0.002$. Therefore, the CLEO II measurement can be interpreted as a measurement of the ratio of form factors $f_+^\pi(0)/f_+^K(0) = 1.29 \pm 0.21 \pm 0.11$ consistent with theoretical predictions which range from 0.7 to 1.4.

5.3 $D^+ \to \bar{K}^{*0} l^+ \nu_l$

One level more complicated than the semileptonic decay of a D meson to a pseudoscalar is the decay to a vector meson. The most easily reconstructed semileptonic D decay to a vector meson is $D^+ \to \bar{K}^{*0} l^+ \nu_l$ with $\bar{K}^{*0} \to K^- \pi^+$. All of the final state particles except the neutrino are charged and hence easily detected. Five independent kinematic variables completely describe this decay. The following five variables are usually used in calculations and analyses: the $l\nu_l$ invariant mass squared q^2; the $K\pi$ invariant mass $m_{K\pi}$; the angle θ_l between the charged lepton and direction opposite that of the $\bar{K}^{*0}$ in the $l\nu_l$ rest frame; the angle θ_V between the K^- and the direction opposite that of the W^+ measured in the $\bar{K}^{*0}$ rest frame; and the angle χ between the decay planes of the $l\nu_l$ and the $K\pi$ systems in the D^+ rest frame. The hadronic matrix element for this decay is constructed from the four-vectors in the decay and Lorentz-invariant form factors that contain the effects of the strong interaction. The available four-vectors can be taken to be the D momentum P, the K^* momentum in the D rest frame K, and the K^* polarization vector ε. Each term in the hadronic matrix element must be linear in ε. The most general matrix element contains both a vector and axial vector part: $\langle K, \varepsilon | V_\mu | P \rangle = -iV(q^2)(M_D + M_{K^*})^{-1} \epsilon_{\mu\nu\rho\sigma} \varepsilon^{*\nu} P^\rho K^\sigma$, and $\langle K, \varepsilon | A_\mu | P \rangle = (M_D + M_{K^*}) A_1(q^2) \varepsilon^*_\mu - A_2(q^2)(M_D + M_{K^*})^{-1} \varepsilon^* \cdot P (P_\mu + K_\mu)$. $V(q^2)$, $A_1(q^2)$ and $A_2(q^2)$ are dimensionless form factors. Pole dominance is usually assumed for the form factors just as with the form factor in $D \to K l \nu_l$ decay discussed in the previous section. This hadronic current is contracted with the leptonic current and the differential decay rate is calculated to be

$$\begin{aligned}
\frac{d\Gamma}{dM^2_{K\pi}\, dq^2\, d\cos\theta_V\, d\cos\theta_l\, d\chi} &= G_F^2 |V_{cs}|^2 \frac{3}{2(4\pi)^5} \frac{m_{K^*}}{m_D^2 m_{K\pi}} K q^2 \\
&\times \frac{m_{K^*}\Gamma}{(m^2_{K\pi} - m^2_{K^*})^2 + m^2_{K^*}\Gamma^2} \\
&\times \{(1+\cos\theta_l)^2 \sin^2\theta_V |H_+(q^2)|^2 \\
&+ (1-\cos\theta_l)^2 \sin^2\theta_V |H_-(q^2)|^2 \\
&+ \sin^2\theta_l 2\cos\theta_V |H_0(q^2)|^2 \\
&- 2\sin^2\theta_l \sin^2\theta_V Re(e^{i2\chi} H_+^* H_-) \\
&- 4\sin\theta_l (1+\cos\theta_l) \sin\theta_V \cos\theta_V Re(e^{i\chi} H_+^* H_0) \\
&+ 4\sin\theta_l (1-\cos\theta_l) \sin\theta_V \cos\theta_V Re(e^{i\chi} H_-^* H_0)\}.
\end{aligned}$$

The form factors are contained in the helicity amplitudes $H_i(q^2)$ that correspond to the three helicity states of the K^*:

$$\begin{aligned}
H_\pm(q^2) &= (m_D + m_{K\pi}) A_1(q^2) \mp \frac{m_D K}{m_D + m_{K\pi}} V(q^2), \\
H_0(q^2) &= \frac{1}{2q m_{K\pi}} [(m_D^2 - m^2_{K\pi} - q^2)(m_D + m_{K\pi}) A_1(q^2) \\
&\quad - 4 \frac{m_D^2 K^2}{m_D + m_{K\pi}} A_2(q^2)].
\end{aligned}$$

Since the form factor $A_1(q^2)$ appears in all three helicity amplitudes, it is usually factored out. Then, an analysis of the distribution of the five kinematic variables yields a measurement of the ratios of form factors $R_V \equiv V(0)/A_1(0)$ and $R_2 \equiv A_2(0)/A_1(0)$.

Measurements of R_V and R_2 have been made by the , E691 [27] E653 [28] and E687 [29] collaborations. In addition, E691 and E653 measured the branching ratio for $D^+ \to \bar{K}^{*0} l^+ \nu_l$ relative to $D^+ \to K^- \pi^+ \pi^+$, allowing them to extract values for all three form factors. The results and the number of events used in each analysis are shown in Table 8. Also shown are the range of theoretical predictions from QCD-inspired phenomenological models, lattice calculations and QCD sum rules. Generally, the measured values of $A_1(0)$ (which dominates the decay rate) and $V(0)$ are low compared to theoretical predictions. However, all the experimental results are consistent with each other given the size of the uncertainties on the measurements. The E791 collaboration expects to have a sample of approximately 2500 candidate $D^+ \to \bar{K}^{*0} e^+ \nu_e$ decays when the entire data sample is analysed [30]. The mode $D^+ \to \bar{K}^{*0} \mu^+ \nu_\mu$ will also be analysed by E791.

Measurements of the branching fraction for $D^+ \to \bar{K}^{*0} l^+ \nu_l$ relative to that for $D^+ \to K^- \pi^+ \pi^+$are summarized in Table 9. The new world average for the

Table 8 Experimental measurements of the ratios of form factors $R_V = V(0)/A_1(0)$ and $R_2 = A_2(0)/A_1(0)$, and of the individual form factors $V(0)$, $A_1(0)$ and $A_2(0)$. Also shown are the range of theoretical predictions for each quantity

Experiment # of events	E691 [27] ~ 200	E653 [28] ~ 300	E657 [29] ~ 900	Theoretical Predictions
R_V	$2.0 \pm 0.6 \pm 0.3$	$2.00^{+0.34}_{-0.32} \pm 0.16$	$1.74 \pm 0.27 \pm 0.28$	1.0–1.9
R_2	$0.0 \pm 0.5 \pm 0.2$	$0.82^{+0.22}_{-0.23} \pm 0.11$	$0.78 \pm 0.18 \pm 0.10$	0.8–1.3
$A_1(0)$	$0.46 \pm 0.05 \pm 0.05$	0.49 ± 0.07		0.5–1.0
$A_2(0)$	$0.0 \pm 0.2 \pm 0.1$	0.4 ± 0.14		0.6–1.2
$V(0)$	$0.9 \pm 0.3 \pm 0.1$	1.0 ± 0.3		1.0–1.5

Table 9 Experimental measurements of the branching fraction for $D^+ \to \bar{K}^{*0}l^+\nu_l$ relative to that for $D^+ \to K^-\pi^+\pi^+$

Experiment	$B(D^+ \to \bar{K}^{*0}l^+\nu_l)/B(D^+ \to K^-\pi^+\pi^+)$
E691 [31]	$0.49 \pm 0.04 \pm 0.05$
ARGUS [32]	$0.55 \pm 0.08 \pm 0.10$
E653 [33]	$0.46 \pm 0.07 \pm 0.08$
E687 [29]	$0.56 \pm 0.04 \pm 0.06$
Average	0.51 ± 0.04

absolute branching fraction for $D^+ \to K^-\pi^+\pi^+$ of $(8.98 \pm 0.83)\%$ yields an absolute branching fraction for $D^+ \to \bar{K}^{*0}l^+\nu_l$ of $(4.58 \pm 0.56)\%$.

The CLEO II experiment [19] has also extracted the following decay rates to a vector meson relative to the rate to a pseudoscalar meson: $\Gamma(D^0 \to K^{*-}l^+\nu_l)/\Gamma(D^0 \to K^-l^+\nu) = 0.60 \pm 0.09 \pm 0.07$ and $\Gamma(D^+ \to \bar{K}^{*0}l^+\nu_l)/\Gamma(D^+ \to \bar{K}^0l^+\nu_l) = 0.65 \pm 0.09 \pm 0.10$. The average of these two ratios is 0.62 ± 0.08, higher than the previous world average of 0.49 ± 0.08, but still lower than the model predictions which lie in the range 0.9 - 1.2.

5.4 $D_s \to \phi l^+\nu_l$

Two studies of the decay $D_s \to \phi l^+\nu_l$ are of interest: the measurement of the branching fraction relative to $D_s \to \phi\pi^+$ that can be used to extract an absolute branching fraction for $D_s \to \phi\pi^+$, and the measurement of the form factors that can be compared to those for $D^+ \to \bar{K}^{*0}l^+\nu_l$ and to theoretical predictions.

Experimental measurements of $\Gamma(D_s \to \phi l^+\nu_l)/\Gamma(D_s \to \phi\pi^+)$ are summarized in Table 10. The average value is 0.54 ± 0.09. The absolute branching fraction for $D_s \to \phi\pi^+$ is related to this measured ratio as follows:

$$B(D_s \to \phi\pi^+) = B(D_s \to \phi l^+\nu_l)\frac{\Gamma(D_s \to \phi\pi^+)}{\Gamma(D_s \to \phi l^+\nu_l)}.$$

We now take advantage of the fact that theory can fairly reliably predict the relative rates for $D_s \to \phi l^+\nu_l$ and $D^+ \to \bar{K}^{*0}l^+\nu_l$. The measured D_s and D^+ lifetimes can be used to relate the decay rates to branching fractions. Therefore, we have the relation $B(D_s \to \phi l^+\nu_l) = F \cdot B(D^+ \to \bar{K}^{*0}l^+\nu_l)\tau_{D_s}/\tau_{D^+}$ where F is the theoretical prediction for $\Gamma(D_s \to \phi l^+\nu_l)/\Gamma(D^+ \to \bar{K}^{*0}l^+\nu_l)$. A value of $F = 0.9 \pm 0.1$ is consistent with the predictions of a number of theorists. Using the value of $B(D^+ \to \bar{K}^{*0}l^+\nu_l) = (4.58 \pm 0.56)\%$ from the previous section and the ratio of lifetimes $\tau_{D_s}/\tau_{D^+} = 0.44 \pm 0.02$, we get the prediction $B(D_s \to \phi\pi^+) = (3.4 \pm 0.7 \pm 0.4)\%$ where the last uncertainty reflects the range of theoretical predictions for F. This is consistent with the upper limit of 4.1% that Mark III obtained from a double-tagging technique [34].

Table 10 Experimental measurements of the branching fraction for $D_s \to \phi l^+\nu_l$ relative to that for $D_s \to \phi\pi^+$

Experiment	# of events	$B(D_s \to \phi l^+\nu_l)/B(D_s \to \phi\pi^+)$
E691 [35]	no signal	< 0.45
ARGUS [32]	104	$0.57 \pm 0.15 \pm 0.15$
CLEO II [36]	54	$0.49 \pm 0.10^{+0.10}_{-0.14}$
E687 [37]	97	$0.58 \pm 0.11 \pm 0.08$
Average		0.54 ± 0.09

Experiment E653 [38] has analysed the distribution of kinematic variables in 24 candidate $D_s \to \phi l^+\nu_l$ decays and extracted the ratio of form factors described in the previous section: $R_2 = 2.1^{+0.6}_{-0.5} \pm 0.2$ and $R_V = 2.3^{+1.1}_{-0.9} \pm 0.4$. The measured value of R_2 is about two standard deviations higher than theoretical predictions.

Experiment E653 [38] also has evidence for the Cabibbo-favored D_s semileptonic decay $D_s \to (\eta \text{ or } \eta')\mu\nu$. They do not reconstruct the π^0's in the η or η' decays, but observe an enhancement in the $\pi^+\pi^-$ mass plot just below the η mass. The signal corresponds to a rate relative to $D_s \to \phi l^+\nu_l$ of $\frac{B(D_s \to (\eta \text{ or } \eta')\mu\nu)}{B(D_s \to \phi\mu\nu)} = 3.9 \pm 1.6$.

6 D_s Lifetime

The E687 collaboration [39] has measured the D_s lifetime with an uncertainty approximately half that of the previously most precise measurement by E691. The D_s lifetime measurements for these two experiments (which are much more precise than any other measurements) are listed in Table 11. The fractional error on the average D_s lifetime is about twice the fractional error on the world averages for the D^0 and the D^+ lifetimes: $\tau_{D^0} = (4.20 \pm 0.08) \times 10^{-13}$ s and $\tau_{D^+} = (10.66 \pm 0.23) \times 10^{-13}$ s. The world average for the ratio of the D_s to the D^0 lifetime (neglecting correlated errors) is $\tau_{D_s}/\tau_{D^0} = 1.11 \pm 0.05$.

Table 11 Experimental measurements of the D_s lifetime

Experiment	D_s lifetime
E691 [40]	$(4.7 \pm 0.4 \pm 0.2) \times 10^{-13}$ s
E687 [39]	$(4.75 \pm 0.20 \pm 0.07) \times 10^{-13}$ s
Average	$(4.74 \pm 0.19) \times 10^{-13}$ s

7 Mixing and Doubly-Cabibbo-Suppressed Decays

Within the Standard Model, the rate of mixing in the $D^0\bar{D}^0$ system is expected to be very small. Hence, the D system is sensitive to effects beyond the Standard Model which can lead to mixing-like signals (flavor-changing neutral currents, charged Higgs, *etc.*).

Before this year, the two most sensitive studies of mixing were conducted by the Mark III [41] and E691 [42] collaborations. Mark III isolated 227 events with two fully reconstructed hadronic decays of neutral D mesons. In three of these events, the strangeness quantum number was the same in both of the D decays. Two possible interpretations of these events are mixing and doubly-Cabibbo-suppressed decays (DCSD). However, a quantum statistics argument can be used to show that mixing must be present if the two D decays in a single event have identical final states. [43] One of the Mark III events is consistent with both D's decaying to $K^-\rho^+$ while the other event is consistent with both decaying to $K^{*0}\pi^0$. However, since the ρ resonance is broad, the D decays in the first event could also be nonresonant decays and, therefore, the event could be due to DCSD rather than mixing. The Mark III collaboration calculates a *lower* limit on the ratio r of D decays to "wrong-sign" strangeness relative to "right-sign" strangeness final states of $r > 0.4\%$ at the 90% confidence level.

The E691 collaboration was able to distinguish DCSD from mixing because of the very precise time resolution afforded by the silicon detectors and the fact that the time evolution of a DCSD signal is purely exponential while that for mixing is an exponential multiplied by t^2. In E691, the charge of the bachelor pion in $D^{*+} \to D^0\pi^+$ is used to identify the original charm quantum number of the D meson. This technique yielded the following *upper* limits under the assumption that there is *no* interference between DCSD and mixing: $r_m < 0.37\%$ and $r_{DCSD} < 1.5\%$ at the 90% confidence level. The limits are not as stringent when interference is allowed.

This year there are two new mixing results. Experiment E687 [44] has used the same technique as E691 to set a limit of $r_m < 0.6\%$ with 10% of their data. The CLEO II experiment [45] observes a signal for $D^0 \to K^+\pi^-$ (a wrong-sign decay) using $D^{*+} \to D^0\pi^+$ to identify the charm quantum number of the D. The wrong-sign signal corresponds to 19 ± 6 events while the number of right-sign events is 2465 ± 50, leading to a measurement of $r = (0.77 \pm 0.25 \pm 0.25)\%$ Since no time-dependence is measured, there is no way to identify this signal as due to mixing or DCSD. Only the expectation that the mixing rate is much smaller allows one to interpret the observed signal as due to DCSD.

8 Summary

With increasing data sample sizes for both e^+e^- and fixed-target experiments, we are seeing significant decreases in statistical errors on measurements which have been limited by data sample sizes in the past—D_s lifetime, $D^0\bar{D}^0$ mixing and DCSD, rare decays, *etc.* In particular, the combination of large samples of charm decays and/or specialized detectors and triggers have led to significant signals for purely leptonic decays in at least three experiments. The excellent photon detection capabilities of the CLEO II detector have opened new areas in charm physics such as $D^* \to D\pi^0$ tagging and reconstruction of $D \to \pi^0 l\nu$. As well as charm decay physics, significant improvements have been made in the study of charmed meson and baryon spectroscopy, and charmed baryon physics in general [46].

REFERENCES

[1] *Charm Decay Physics*, M.S.Witherell, preprint UCSB-HEP-93-06, Invited talk given at the International Symposium on Lepton and Photon Interactions at High Energies, Cornell University, Ithaca, NY, August, 1993.

[2] CLEO II Collaboration, F. Butler *et al.*, Phys. Rev. Lett. 69, 2041 (1992).

[3] Particle Data Group, K. Hikasa *et al.*, Phys. Rev. D 45, No. 11, Pt. II (1992).

[4] For example, see L. Angelos and G. P. Lepage, Phys. Rev. D 45, R3021 (1992).

[5] Mark III Collaboration, J.Adler *et al.*, Phys. Lett. B208, 152 (1988).

[6] CLEO II Collaboration, D. Bortoletto *et al.*, Phys. Rev. Lett. 69, 2046 (1992).

[7] Mark III Collaboration, J. Adler *et al.*, Phys. Rev. Lett. 60, 89 (1988).

[8] ACCMOR Collaboration, S. Barlag *et al.*, Z. Phys. C 55, 383 (1992); Z. Phys. C 48, 29 (1990).

[9] HRS Collaboration, S. Abachi *et al.*, Phys. Lett. B205, 411 (1988).

[10] ALEPH Collaboration, D. Decamp *et al.*, Phys. Lett. B266, 218 (1991).

[11] ALEPH Collaboration, contribution to International Symposium on Lepton and Photon Interactions at High Energies, Cornell University, Ithaca, NY, August, 1993.

[12] CLEO II Collaboration. For the D^0 measurement, D.S.Akerib *et al.*, CLEO preprint CLEO 93-16 (1993), submitted to Phys. Rev. Lett.; for the D^+ measurement, see contribution by H.Yamamoto to these proceedings.

[13] ARGUS Collaboration, contribution to International Symposium on Lepton and Photon Interactions at High Energies, Cornell University, Ithaca, NY, August, 1993.

[14] Mark III Collaboration, J.Adler *et al.*, Phys. Rev. Lett. 60, 1375 (1988).

[15] EMC Collaboration, J.J.Aubert *et al.*, Nucl. Phys. B213, 31 (1983).

[16] WA75 Collaboration, S.Aoki *et al.*, Prog. Theor. Phys. 89, 131 (1993).

[17] E653 Collaboration, contribution to International Symposium on Lepton and Photon Interactions at High Energies, Cornell University, Ithaca, NY, August, 1993.

[18] CLEO II Collaboration, FY.Kubota *et al.*, preprint CLEO 93-14, submitted to Phys. Rev. D (1993); also contribution by F.Muheim to these proceedings.

[19] CLEO II Collaboration, A.Bean *et al.*, CLEO preprint CLEO 93-18, submitted to Phys. Lett. B (1993).

[20] Mark III Collaboration, Z.Bai *et al.*, Phys. Rev. Lett. 66, 1011 (1991).

[21] E691 Collaboration, J.C.Anjos *et al.*, Phys. Rev. Lett. 62, 1587 (1989).

[22] CLEO Collaboration, G.Crawford *et al.*, Phys. Rev. D44, 3394 (1991).

[23] E687 Collaboration, P.L.Frabetti *et al.*, Phys. Lett. B315, 203 (1993).

[24] N.Isgur, D.Scora, B.Grinstein, M.Wise, Phys. Rev. D 39, 799 (1989).

[25] CLEO II Collaboration, M.S.Alam *et al.*, Phys. Rev. Lett. 71, 1311 (1993).

[26] Mark III Collaboration, J.Adler *et al.*, Phys. Rev. Lett. 62, 1821 (1989).

[27] E691 Collaboration, J.C.Anjos *et al.*, Phys. Rev. Lett. 65, 2630 (1990).

[28] E653 Collaboration, K.Kodama *et al.*, Phys. Lett. B274, 246 (1992).

[29] E687 Collaboration, P.L.Frabetti *et al.*, Phys. Lett. B307, 262 (1993).

[30] E791 Collaboration, see contribution by P.Gagnon to these proceedings.

[31] E691 Collaboration, J.C.Anjos *et al.*, Phys. Rev. Lett. 62, 722 (1989).

[32] ARGUS Collaboration, H.Albrecht *et al.*, Phys. Lett. B255, 634 (1991).

[33] E653 Collaboration, K.Kodama *et al.*, Phys. Lett. B286, 187 (1992).

[34] Mark III Collaboration, J.Adler *et al.*, Phys. Rev. Lett. 64, 169 (1990).

[35] E691 Collaboration, J.C.Anjos *et al.*, Phys. Rev. Lett. 64, 2885 (1990).

[36] CLEO II Collaboration, J.Alexander *et al.*, Phys. Rev. Lett. 65, 1531 (1990).

[37] E687 Collaboration, P.L.Frabetti *et al.*, Phys. Lett. B313, 253 (1993).

[38] E653 Collaboration, K.Kodama *et al.*, Phys. Lett. B309, 483 (1993).

[39] E687 Collaboration, P.L.Frabetti *et al.*, Phys. Rev. Lett. 71, 827 (1993).

[40] E691 Collaboration, J.Raab *et al.*, Phys. Rev. D 37, 2391 (1988).

[41] Mark III Collaboration, G.Gladding, Proceedings of the International Symposium on Production and Decay of Heavy Flavors, Stanford, 1988.

[42] E691 Collaboration, J.C.Anjos *et al.*, Phys. Rev. Lett. 60, 1239 (1988).

[43] I.Bigi and A.I.Sanda, Phys. Lett. B171, 320 (1986).

[44] E687 Collaboration, private communication.

[45] CLEO II Collaboration, contribution by H.Yamamoto to these proceedings.

[46] For example, see contributions to these proceedings by A.Zallo (E687), R.Van de Water (ARGUS) and M.Procario (CLEO).